Mem. S.A.It. Vol. 88, 761

Memorie della

Grain growth in Class I protostar Per-emb-50: a dust continuum analysis with NOEMA & SMA

C. Agurto-Gangas[1], J. E. Pineda[1], L. Testi[2,3,4], P. Caselli[1], L. Szűcs[1], M. Tazzari[5], M. Dunham[6], I. W. Stephens[7], and A. Miotello[8]

[1] Max-Planck-Institute for Extraterrestrial Physics (MPE), Giessenbachstr. 1, D-85748 Garching, Germany, e-mail: cagurto@mpe.mpg.de
[2] ESO, Karl Schwarzschild str. 2, D-85748 Garching, Germany
[3] INAF-Osservatorio Astrofisico di Arcetri, L.go E. Fermi 5, Firenze, 50125, Italy
[4] Excellence Cluster Universe, Boltzmannstr. 2, D-85748 Garching, Germany
[5] Institute of Astronomy, Madingley Road, Cambridge, CB3 0HA, UK
[6] Department of Physics, State University of New York at Fredonia, 280 Central Ave, Fredonia, NY 14063
[7] Harvard-Smithsonian Center for Astrophysics, 60 Garden Street, Cambridge, MA 02138, USA
[8] Leiden Observatory, Leiden University, P.O. Box 9513, NL-2300 RA, Leiden, The Netherlands

Abstract. A good understanding of when dust grains grow from sub-micrometer to millimeter sizes occurs is crucial for models of planet formation. This provides the first step towards the production of pebbles and planetesimals in protoplanetary disks. Thanks to detailed studies of the spectral index in Class II disks, it is well established that Class II objects have already dust grains of millimetres sizes, however, it is not clear when in the star formation process this grain growth occurs. Here, we present interferometric data from NOEMA at 3 mm and SMA at 1.3 mm of the Class I protostar, Per-emb-50, to determine the flux density spectral index at mm-wavelengths of the unresolved disk and the surrounding envelope. We find a spectral index in the unresolved disk 30% smaller than the envelope, α_{env}=2.18, comparable to values obtained toward Class 0 sources.

1. Introduction

Disks and envelopes around protostars play a fundamental role in the process of planet formation, since they contain the ingredients which could be used later to form planets (Testi et al. 2014). Thanks to detailed studies on protoplanetary disks such as: HL Tau (ALMA Partnership et al. 2015)), it is now well established that Class II objects have already dust grains of millimeter sizes. However, it is not yet clear at which stage of the star and planet formation process dust grains start to efficiently coagulate and evolve from μm dust size particles to macroscopic dimensions. Here we present new millimeter observations of Per-emb-50, a Class I protostar in the Perseus star forming region (SFR).

2. SMA & NOEMA data

Per-emb-50 is a protostar located in the active cluster forming region NGC1333 at a distance

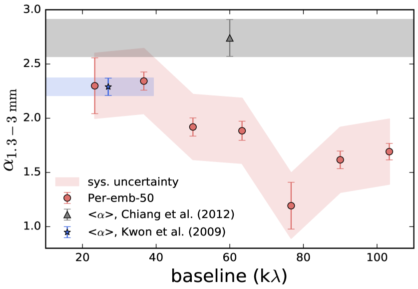

Fig. 1. Flux density spectral index α_{mm} between 1.3 mm and 3 mm as a function of deprojected baseline. The red dots represent the α_{mm} for Per-emb-50, where the error bars show the statistical errors and the red shaded region indicates a systematic calibration uncertainty of 0.3. As comparison, average $< \alpha_{mm} >$ from two Class 0 protostars are plotted: gray dot and shadow region is $< \alpha_{mm} >$ and systematic uncertainty of L1157 (Chiang et al. 2012), while the blue dot represent the $< \alpha_{mm} >$ of L1448 IRS 3B from Kwon et al. (2009)).

of 235±18 pc (Hirota et al. 2008). It was observed in both: 1.3 mm and 3 mm. The 1.3 mm SMA data was taken in sub-compact and extended configuration as part of the MASSES program, PIs: I.W. Stephens, M. Dunham. While the 3mm observations were carried out with the recently upgraded NOEMA in C configuration. Both set of data provide an angular resolution of 2.”0×1.”5 and are sensitive to scales down to 400 AU.

3. Preliminary results

Flux density spectral index α_{mm} is related to dust emissivity spectral index β_{mm} via α_{mm}=β_{mm}+2 (valid in the optically thin assumption and the Rayleigh-Jeans (RJ) approximation), and can be calculated by observations at two frequencies with the following relation: α_{mm}=(ln F_1 - ln F_2)/(ln ν_1 - ln ν_2) + 2. Per-emb-50 consists of two components, an envelope and a disk. Since it is possible that envelope and disk emission are better described with different spectral indexes, we decide to model the emission with two components with different α_{mm}. We derived a flux density spectral index from the excess emission at shorter baselines (<60 kλ) of 2.18±0.12, while the spectral index relative to the unresolved disk is 1.61±0.11 (see Fig. 1). The lower values of flux density spectral indexes α_{mm} in this work are affected by the unresolved disk, therefore, in order to recover the interferometer fluxes at very short baselines and obtain α_{mm} through the envelope, subtraction of the disk visibilities from the total visibilities are needed.

4. Conclusion

We present new 3 mm NOEMA data and 1.3 mm SMA data of the Class I protostar in the Perseus SFR: Per-emb-50. From the analysis in the uv plane we can detect the presence of two contributions: an extended envelope related with an increase of the fluxes at short baselines and a constant non-zero emission at the long baselines, which shows the presence of an unresolved disk. Fig. 1 shows a differentiation of the flux density spectral index between disk and envelope, where $< \alpha_{disk} >$ is a 30% smaller than $< \alpha_{env} >$. Previous studies on Class 0/I sources suggest that dust grains start to aggregate up to mm sizes already in the envelope, showing spectral indexes similar to our source. However, the envelope flux density spectral index presented here can be highly affected by the emission of the unresolved disk at shortest baselines and result in spectral indexes lower than the ISM values (α_{ISM}=3.7). Therefore, subtraction of the disk visibilities from the total visibilities at short baselines are needed to recover an reliable envelope spectral index. Additionally, a proper radiative transfer modeling of both structures is needed to explore possible scenarios for the interpretation of the source and to determine α_{mm}.

References

ALMA Partnership, et al. 2015, ApJL, 808, 1
Chiang, H.-F., et al. 2012, ApJ, 756, 168
Kwon, W., et al. 2009, ApJ, 696, 841
Testi, L. et al. 2014, Prot. and Plan. VI, p. 339
Hirota, T. et al. 2008, PASJ, 60, 37